

Locating the Launching Region of T Tauri Winds: The Case of DG Tau

Jeffrey M. Anderson and Zhi-Yun Li

*Department of Astronomy, University of Virginia, P. O. Box 3818, Charlottesville, VA
22903*

jma2u@virginia.edu, zl4h@virginia.edu

Ruben Krasnopolsky

*Center for Theoretical Astrophysics, University of Illinois at Urbana-Champaign, Loomis
Laboratory, 1110 West Green Street, Urbana, IL 61801*

ruben@astro.uiuc.edu

Roger D. Blandford

*California Institute of Technology, Theoretical Astrophysics, 130-30 Caltech, Pasadena, CA
91125*

rdb@tapir.caltech.edu

ABSTRACT

It is widely believed that T Tauri winds are driven magnetocentrifugally from accretion disks close to the central stars. The exact launching conditions are uncertain. We show that a general relation exists between the poloidal and toroidal velocity components of a magnetocentrifugal wind at large distances and the rotation rate of the launching surface, independent of the uncertain launching conditions. We discuss the physical basis of this relation and verify it using a set of numerically-determined large-scale wind solutions. Both velocity components are in principle measurable from spatially resolved spectra, as has been done for the extended low-velocity component (LVC) of the DG Tau wind by Bacciotti et al. For this particular source, we infer that the spatially resolved LVC originates from a region on the disk extending from ~ 0.3 to ~ 4.0 AU from the star, which is consistent with, and a refinement over, the previous rough estimate of Bacciotti et al.

Subject headings: ISM: jets and outflows — magnetohydrodynamics — stars: formation — stars: individual: DG Tau — stars: pre-main sequence

1. INTRODUCTION

The magnetocentrifugal mechanism (Blandford & Payne 1982) is widely considered the leading candidate for producing jets and winds in star formation (see reviews by Königl & Pudritz 2000; Shu et al. 2000); alternative mechanisms involving thermal and/or radiation pressure have been shown to be inadequate. An outflow can in principle be launched by torsional Alfvén waves, as shown numerically by Shibata & Uchida (1985) and others (see Kato, Kudoh, & Shibata 2002 and references therein). These simulations are typically of relatively short duration, however, and it is not clear whether a large-scale, sustained outflow can be produced by this mechanism alone.

The magnetocentrifugal model has two popular versions: X-winds (Shu et al. 2000) and disk-winds (Königl & Pudritz 2000). The X-winds are launched from a narrow region close to the truncation radius R_X of the Keplerian disk by a stellar magnetosphere. The disk-winds are, on the other hand, envisioned to come from a wider range of disk radii outside R_X . These two possibilities are not immediately distinguishable observationally, because the launching surfaces in both cases are thought to be small, and only the flow regions at much larger distances are directly observable at the present.

In this Letter, we derive a method of inferring the rotation rate (and thus the radius) of the wind-launching region on the Keplerian disk from measurable quantities at large distances (§2). In §3, we first test the method on a set of numerically-determined large-scale magnetocentrifugal wind solutions, and then apply it to the well-studied wind of the T Tauri star DG Tau, using data obtained by Bacciotti et al. (2002) with the Space Telescope Imaging Spectrograph (STIS) of the *Hubble Space Telescope* (HST). We discuss our results and conclude in §4.

2. A METHOD FOR LOCATING THE WIND-LAUNCHING REGION

2.1. Physical Basis of the Method

The basic principle of magnetocentrifugal wind launching is well understood. It involves open field lines firmly anchored on a rapidly rotating disk, and centrifugal acceleration of fluid parcels along the field lines into a high-speed wind. The wind trails behind the disk in rotation, generating a toroidal component of magnetic field, which exerts a braking torque on the disk. It is this magnetic torque that is responsible for extracting both energy and angular momentum from the disk and for powering the wind. Since the energy extracted is simply the work done by the rotating disk against the magnetic torque (e.g. Spruit 1996),

the rate of energy extraction is directly proportional to the rate of angular momentum extraction, with the proportionality constant being the angular speed Ω_0 of the disk rotation. The extracted energy and angular momentum are initially stored in an electromagnetic form. They are gradually converted into a kinetic form as the flow accelerates. At large observable distances, the conversion is nearly complete, and the wind becomes kinetically dominated. Along any given field line, the kinetic energy will then be proportional to the fluid angular momentum, with the same proportionality constant Ω_0 because of energy and angular momentum conservation.

At any observable location (say of a distance ϖ_∞ from the rotation axis, where the subscript denotes a quantity far from the launching region), the specific kinetic energy and angular momentum of the wind are given by the poloidal and toroidal components of the fluid velocity, $v_{p,\infty}$ and $v_{\phi,\infty}$, through $(v_{p,\infty}^2 + v_{\phi,\infty}^2)/2$ and $v_{\phi,\infty}\varpi_\infty$ respectively. Both velocity components can in principle be derived empirically from spatially resolved spectra and proper motion observations, as has been done for DG Tau (Bacciotti et al. 2002). Once measured, they can be used to deduce the rate of disk rotation at the foot point of the field line passing through that location, through

$$\Omega_0 \approx \frac{v_{p,\infty}^2/2}{v_{\phi,\infty}\varpi_\infty}, \quad (1)$$

where $v_{\phi,\infty} \ll v_{p,\infty}$ is assumed, as is generally true at large distances. The above relation provides a simple way to infer the rotation rate of the wind-launching region on the Keplerian disk and, if the central stellar mass is known independently, the distance from the star. In the next subsection, we will use the steady magnetohydrodynamic (MHD) wind theory to derive a refined version of this relation, taking into account of the energy and angular momentum associated with fluid rotation at the base of the wind.

2.2. General Derivation

It is well known that in a steady, axisymmetric MHD wind, several quantities are conserved along a given field line (Mestel 1968). These include the total specific energy and angular momentum

$$E = \frac{v^2}{2} - \frac{B_\phi B_p \Omega \varpi}{4\pi\rho v_p} + h + \Phi_g, \quad L = \varpi \left(v_\phi - \frac{B_\phi B_p}{4\pi\rho v_p} \right), \quad (2)$$

and the quantity $\Omega = (v_\phi - B_\phi v_p/B_p)/\varpi$, which can be interpreted as the angular speed at the base of the wind, Ω_0 , where the poloidal flow speed v_p is negligible compared to the speed of Keplerian rotation. Here, v denotes velocity, B magnetic field, h specific enthalpy, ρ mass density, and Φ_g the gravitational potential. The subscript p refers to a quantity in the

poloidal (ϖ, z) plane of a cylindrical coordinate system (ϖ, ϕ, z) . We will ignore the enthalpy term in the expression for specific energy since magnetocentrifugal winds are dynamically cold in general.

Note from equation (2) that the magnetic contributions to the energy and angular momentum are proportional to each other. Since neither of them can be measured directly, we get rid of both by constructing a combined quantity

$$J \equiv E - \Omega L = \frac{v^2}{2} + \Phi_g - \Omega \varpi v_\phi, \quad (3)$$

which is also conserved along a field line (see also Lovelace et al. 1986). At the launching surface, the wind corotates with the disk at the local Keplerian speed $v_{K,0}$, which yields $J = -3v_{K,0}^2/2$. As the distance increases, the gravitational potential Φ_g decreases quickly, and we have approximately

$$\frac{v_{p,\infty}^2 + v_{\phi,\infty}^2}{2} - \Omega_0 \varpi_\infty v_{\phi,\infty} \approx -\frac{3}{2}v_{K,0}^2. \quad (4)$$

Since the Keplerian speed of disk rotation is related to the angular speed through $v_{K,0} = (GM_*\Omega_0)^{1/3}$ around a star of mass M_* , we finally have

$$\varpi_\infty v_{\phi,\infty} \Omega_0 - \frac{3}{2}(GM_*)^{2/3} \Omega_0^{2/3} - \frac{v_{p,\infty}^2 + v_{\phi,\infty}^2}{2} \approx 0, \quad (5)$$

which is the desired equation for determining the disk rotation rate Ω_0 in the wind-launching region from measurable quantities at large distances.

Mathematically, we can define $\xi \equiv \Omega_0^{1/3}$, and cast equation (5) into a cubic equation

$$\xi^3 - a_2 \xi^2 - a_0 = 0, \quad (6)$$

with the coefficients

$$a_2 = \frac{3}{2} \frac{(GM_*)^{2/3}}{\varpi_\infty v_{\phi,\infty}}, \quad \text{and} \quad a_0 = \frac{v_{p,\infty}^2 + v_{\phi,\infty}^2}{2\varpi_\infty v_{\phi,\infty}}. \quad (7)$$

If we let $q = -a_2^2/9$, $r = a_0/2 + a_2^3/27$, and $D = q^3 + r^2 = a_0^2/4 + a_2^3 a_0/27$, then the nature of the solution is determined by the value of D . For $D > 0$, which is always true in our case, there are one real and two complex conjugate roots. The real root is given analytically by

$$\xi = (r + \sqrt{D})^{1/3} + (r - \sqrt{D})^{1/3} + a_2/3. \quad (8)$$

Once ξ is determined, one can obtain the angular speed through $\Omega_0 = \xi^3$, and infer the wind-launching radius through $\varpi_0 = (GM_*/\Omega_0^2)^{1/3}$.

Astrophysically interesting magnetocentrifugal winds are probably “fast” in the sense that they have enough energy to climb out the potential well of the central star easily (instead of barely). In such a case, we expect the kinetic energy of the wind (the third term of eq. [5]) to be substantially greater than the gravitational binding energy at the launching surface (which is essentially the second term of eq. [5]). Noting again that typically $v_{\phi,\infty} \ll v_{p,\infty}$, we recover from equation (5) the simple relation (1), which can be cast into a more practical form

$$\varpi_0 \approx 0.7 \text{ AU} \left(\frac{\varpi_\infty}{10 \text{ AU}} \right)^{2/3} \left(\frac{v_{\phi,\infty}}{10 \text{ km s}^{-1}} \right)^{2/3} \left(\frac{v_{p,\infty}}{100 \text{ km s}^{-1}} \right)^{-4/3} \left(\frac{M_*}{1 M_\odot} \right)^{1/3} \quad (9)$$

for locating the wind-launching region on the disk.

3. METHOD VERIFICATION AND APPLICATION

3.1. Method Verification using Numerical Solutions

We have tested the method of inferring the rotation rate of the wind-launching surface on a set of numerically-determined magnetocentrifugal wind solutions (J. Anderson et al. 2003, in preparation). These solutions are obtained using the ZEUS3D MHD code (Clarke, Norman, & Fiedler 1994) assuming axisymmetry. The simulation setup and code modifications are described in Krasnopolsky, Li, & Blandford (1999). Basically, we prescribe on the Keplerian disk around a solar-mass star a distribution of open magnetic field, and load onto the field a mass flux at a low speed (typically 10% of Keplerian). The slowly-moving wind material is accelerated centrifugally along the rotating field lines into a high-speed flow. The wind gradually sweeps the ambient medium out of the simulation box, chosen to have a 100×100 AU size, and settles into a steady state. The properties of the steady wind at large distances are determined uniquely by the conditions on the launching surface. They are used for our method verification.

The results of applying our method to two representative simulations are presented in Table 1. The simulations differ only in the mass loading rate of the wind; model L corresponds to a “light” wind, with $\dot{M}_w = 10^{-8} M_\odot \text{ yr}^{-1}$, typical of T Tauri winds, and model H corresponds to a “heavy” wind, with $\dot{M}_w = 10^{-6} M_\odot \text{ yr}^{-1}$, which is more extreme (Edwards, Ray, & Mundt 1993). For each model, we first read out from the solution the two velocity components $v_{p,\infty}$ and $v_{\phi,\infty}$ at four selected, observable locations with known cylindrical radius ϖ_∞ , and then compute the corresponding angular speed at the launching surface from both the simple relation (1), $\Omega_{0,A}$, and the refined relation (5), $\Omega_{0,B}$. Comparing the predicted values with the exact Ω_0 , we find that the simple relation (1) works well for the light wind, but under predicts the rotation rate by a factor of two for the more extreme,

heavy wind. The large discrepancy in the latter case comes from the neglect of the fluid energy and angular momentum at the base of the wind in deriving relation (1), which are comparable to their magnetic counterparts for the heavy wind. The fluid contributions are included in relation (5), which yields a rotation rate accurate to within about 5% in both cases. The small errors can be further reduced if the (slow) speed with which the wind solution is initiated and the gravitational binding energy at the observing location are accounted for properly, which can be done. Such refinements are not warranted, however, given the large uncertainties in real observational data, to which we now turn.

3.2. The Case of DG Tau

Observational data needed to locate the wind-launching region on the disk are available for DG Tau, thanks to the spatially resolved spectra of several forbidden lines obtained by Bacciotti et al. (2000) using HST/STIS. The STIS slit was placed along the axis of the flow and at three pairs of locations at distances 10, 20, and 30 AU from the axis (one on each side). Two distinct velocity components are detected, with the high-velocity component (HVC) concentrating near the axis and the low-velocity component (LVC) being more laterally extended. Bacciotti et al. (2002) analyzed the extended LVC in detail, and derived the radial (line-of-sight) velocity $v_{r,\infty}$ at four positions along each slit, labeled I through IV in their Fig. 7. They also found tentative evidence for rotation from the difference in radial velocity between the regions displaced symmetrically with respect to the axis. The axis is inclined at $\theta \approx 38^\circ$ to our line of sight (Eislöffel & Mundt 1998), which allows us to estimate the poloidal speed $v_{p,\infty} = v_{r,\infty} / \cos \theta$, assuming a flow predominantly parallel to the axis. This assumption is expected to break down badly in region I, which is the closest to the disk; it should be accurate to $\sim 50\%$ or better in the other regions. The estimated values of $v_{p,\infty}$ in regions II through IV are listed in Table 2, along with the deprojected toroidal velocities computed using the numbers given in Table 1 of Bacciotti et al. (2002), which are uncertain. The angular speed Ω_0 in Table 2 is derived from equation (5), and the wind-launching radius ϖ_0 is computed for a stellar mass $M_* = 0.67 M_\odot$ (Hartigan et al. 1995).

It is clear from Table 2 that the LVC of the DG Tau wind comes from a range in disk radius, from ~ 0.3 to ~ 4 AU. The spread in launching radius can be understood qualitatively as follows: in each of the three regions, the flow located closest to the axis (at the 10 AU distance) has the highest poloidal speed (and thus the highest specific energy) and the lowest, or close to the lowest, toroidal speed (and thus the lowest specific angular momentum given its small distance). To extract the highest energy against the weakest torque on the disk (corresponding to the lowest angular momentum), the field line passing

through the innermost location in each region must be driven at the fastest rate at the foot point, i.e., must be anchored closest to the central star. Detailed calculations confirm this expectation, as shown in Fig. fig:dgtau, where straight lines connecting the observing locations and their originating points on the disk are plotted. These lines give a crude indication of the actual streamlines. They are well behaved, with two exceptions: the lines associated with the two outer locations in region IV cross other lines, which is problematic. However, region IV appears to be perturbed by a limb-brightened bubble-like structure (Bacciotti et al. 2000), which may have introduced additional asymmetry to the flow with respect to the axis, and compromised the estimates of toroidal speed and thus the foot point locations.

We reiterate that our values of $v_{p,\infty}$ are estimated from the radial velocities at the peak of forbidden lines, which sample only the component of poloidal velocity parallel to the axis, $v_{z,\infty}$, in the likely case of peak emission originating from the tangent point of our line of sight with the wind. Since the v_{ϖ} component is unmeasured, our values of $v_{p,\infty}$ are actually underestimates. This effect will be most pronounced for the least collimated part of the flow, where $v_{p,\infty}$ can be underestimated by as much as $\sim 50\%$. Taking this effect into account could move the outermost launching point inward by a factor up to two.

With the rotation rate Ω_0 determined, we can estimate the Alfvén radius ϖ_A by equating the fluid angular momentum at large distances, $\varpi_{\infty}v_{\phi,\infty}$, with the total angular momentum, $L \equiv \Omega_0\varpi_A^2$ (e.g. Spruit 1996). The estimates for ϖ_A are listed in Table 2 and the corresponding “Alfvén points” are plotted in the right panel of Fig. fig:dgtau. The Alfvén radius turns out to be ~ 1.8 to ~ 2.6 times the foot point radius (except for the “streamline” passing through the bubble-affected outermost location in region IV; see Table 2). The typical ratio of $\varpi_A/\varpi_0 \sim 2$ implies that roughly 1/4 of the material accreted through the disk is ejected in the extended LVC of the DG Tau wind as per the relationship $\dot{M}_w/\dot{M}_d \approx (\varpi_0/\varpi_A)^2$ (Pelletier & Pudritz 1992).

4. CONCLUSIONS AND DISCUSSION

We have developed a method of locating the launching region of T Tauri winds, if such winds are driven magnetocentrifugally, as is widely believed. Our method relies on the fact that the energy and angular momentum in the wind are extracted mostly by magnetic fields from the rotating disk, and they are related by the rate of disk rotation because the energy extracted is the work done by the rotating disk against the magnetic torque responsible for the angular momentum extraction. Since most of the wind energy and angular momentum at large, observable distances are in the measurable kinetic form, they can be used to infer

the disk rotation rate in the wind launching region. Applying this method to the wind of DG Tau, we find that its spatially resolved LVC comes from a region on the disk extending from ~ 0.3 and ~ 4 AU from the central star. This range brackets the rough estimate of ~ 1.8 AU by Bacciotti et al. (2002). It strengthens the notion that the LVCs of T Tauri winds are driven from relatively large disk radii (Kwan & Tademaru 1988).

The DG Tau wind has a HVC with a radial velocity of $\sim 220 \text{ km s}^{-1}$ (Pyo et al. 2003). Where this component is launched is less certain. It is unresolved in the transverse direction in the HST observations (Bacciotti et al. 2000), implying a half-width $\lesssim 5$ AU. Unless rotating at a speed much greater than that inferred for the LVC ($\sim 10 \text{ km s}^{-1}$), the HVC must be driven magnetocentrifugally from a disk region with radius on the order of 0.1 AU or smaller, according to equation (9). The small launching radius is indicative of an X-wind origin (Shu et al. 2000). To draw a more quantitative conclusion on the launching radius of the HVC, its rotational speed must be measured, which may become possible with the advent of optical interferometry using large, ground-based telescopes.

Support for this work was provided in part by NASA grants NAG 5-7007, 5-9180, 5-12102 and NSF grant AST 00-93091.

REFERENCES

- Bacciotti, F., Mundt, R., Ray, T. P., Eisloffel, J., Solf, J., & Camezind, M. 2000, *ApJ*, 537, L49
- Bacciotti, F., Ray, T. P., Mundt, R., Eisloffel, J., & Solf, J. 2002, *ApJ*, 576, 222
- Blandford, R. D., & Payne, D. G. 1982, *MNRAS*, 199, 883
- Clarke, D. A., Norman, M. L., & Fiedler, R. A. 1994, *ZEUS3D User Manual*, <http://zeus.ncsa.uiuc.edu/lca/zeus3d/manuals/>
- Edwards, S., Ray, T., & Mundt, R. 1993, in *Protostars and Planets III*, ed. E. H. Levy & M. S. Matthews (Tuscon: Univ. Arizona Press), 567
- Eisloffel, J., & Mundt, R. 1998, *AJ*, 115, 1554
- Hartigan, P., Edwards, S., & Gandhour, L. 1995, *ApJ*, 452, 736
- Kato, S. X., Kudoh, T., & Shibata, K. 2002, *ApJ*, 565, 1035

Königl, A., & Pudritz, R. E. 2000, in *Protostars and Planets IV*, ed. V. Mannings, A. P. Boss, & S. S. Russell (Tuscon: Univ. Arizona Press), 759

Krasnopolsky, R., Li, Z.-Y., & Blandford, R. 1999, *ApJ*, 526, 631

Kwan, J., & Tademaru, E. 1988, *ApJ*, 332, L41

Lovelace, R. V. E., Mehanian, C., Mobarry, C. M., Sulkanen, M. E. 1986, *ApJS*, 62, 1

Mestel, L. 1968, *MNRAS*, 138, 359

Pelletier, G., & Pudritz, R. E. 1992, *ApJ*, 394, 117

Pyo, T.-S., et al. 2003, *ApJ*, in press

Shibata, K., & Uchida, Y. 1985, *PASJ*, 37, 31

Shu, F. H., Najita, J. R., Shang, H., & Li, Z.-Y. 2000, in *Protostars and Planets IV*, ed. V. Mannings, A. P. Boss, & S. S. Russell (Tuscon: Univ. Arizona Press), 789

Spruit, H. C. 1996, *Evolutionary Processes in Binary Stars*, NATO ASI Series C., 477, 249

.

.

This preprint was prepared with the AAS L^AT_EX macros v5.0.

Table 1. Predicted Ω_0 for Model Calculation

Model	ϖ_0 (AU)	Ω_0 (s ⁻¹)	ϖ_∞ (AU)	$v_{\phi,\infty}$ (km s ⁻¹)	$v_{p,\infty}$ (km s ⁻¹)	$\Omega_{0,A}$ (s ⁻¹)	$\Omega_{0,B}$ (s ⁻¹)
L	0.21	2.16×10^{-6}	20.0	23.0	526.8	2.02×10^{-6}	2.11×10^{-6}
	0.31	1.23×10^{-6}	37.2	15.0	437.3	1.15×10^{-6}	1.20×10^{-6}
	0.40	8.18×10^{-7}	57.1	10.9	377.5	7.67×10^{-7}	8.02×10^{-7}
	0.51	5.66×10^{-7}	90.4	7.6	326.8	5.22×10^{-7}	5.45×10^{-7}
H	0.21	2.10×10^{-6}	11.5	3.6	116.1	1.09×10^{-6}	2.13×10^{-6}
	0.31	1.21×10^{-6}	25.7	2.0	97.7	6.31×10^{-7}	1.19×10^{-6}
	0.40	8.06×10^{-7}	42.9	1.3	83.9	4.14×10^{-7}	8.38×10^{-7}
	0.51	5.60×10^{-7}	69.8	0.9	71.8	2.77×10^{-7}	5.55×10^{-7}

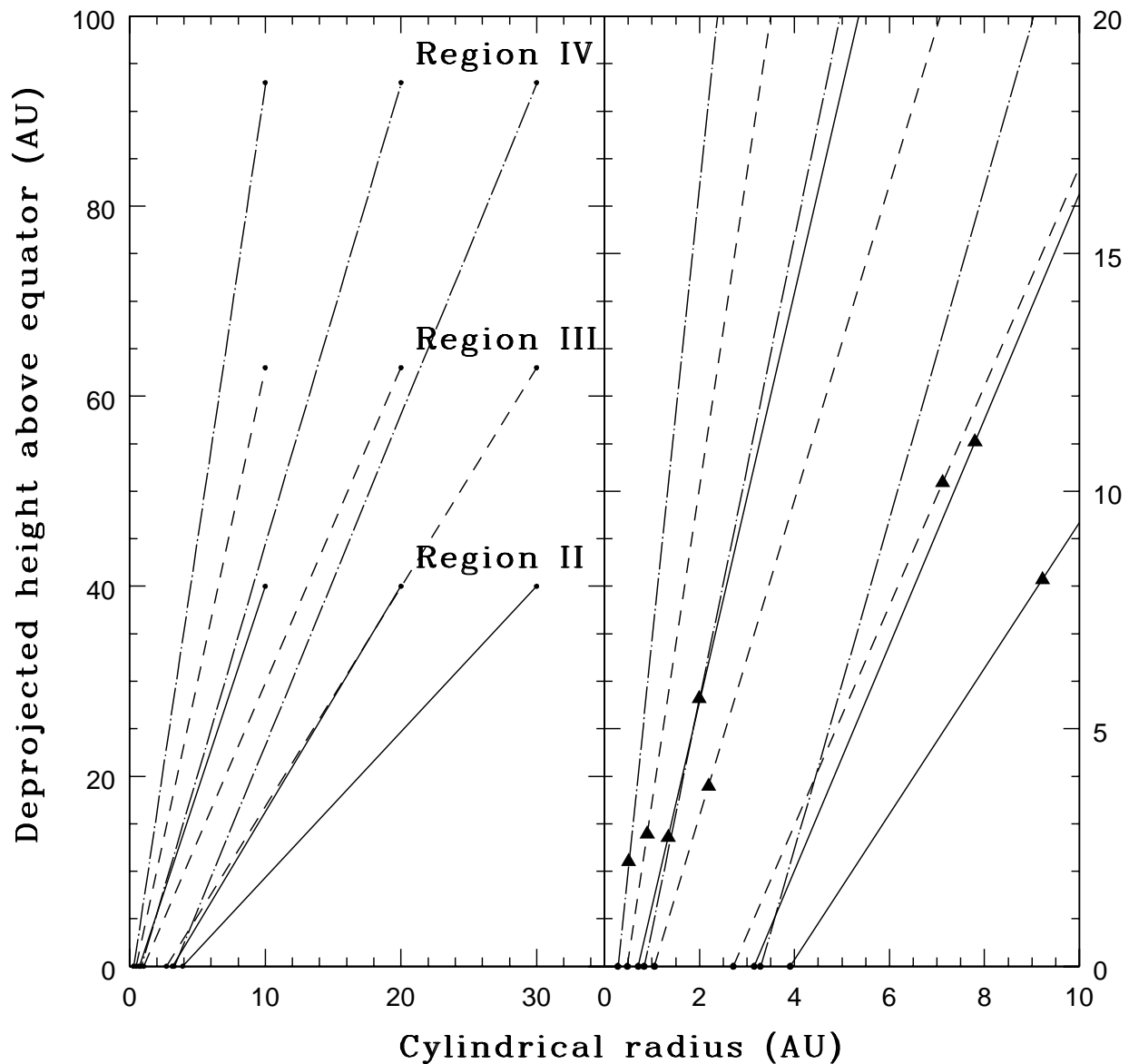


Fig. 1.— Calculated “streamlines” for DG Tau. The left panel shows the observation points from Region II (solid lines), III (dashed), and IV (dash-dotted) of Bacciotti et al. (2002) connected to the calculated foot points of the flow. The right panel is a blow-up of the inner region of the flow, showing where the flow originates from the disk. Also shown on the right panel is the location of the Alfvén surface along each “streamline” as filled triangles.

Table 2. Predicted Ω_0 , ϖ_0 and ϖ_A for LVC of DG Tau Wind

Region	ϖ_∞ (AU)	$v_{\phi,\infty}$ (km s ⁻¹)	$v_{p,\infty}$ (km s ⁻¹)	Ω_0 (s ⁻¹)	ϖ_0 (AU)	ϖ_A (AU)	ϖ_A/ϖ_0
II	10	7.3	58.2	2.7×10^{-7}	0.71	1.34	1.9
	20	13.2	39.5	2.9×10^{-8}	3.15	7.80	2.5
	30	8.9	33.9	2.1×10^{-8}	3.91	9.22	2.4
III	10	5.8	68.5	4.8×10^{-7}	0.48	0.90	1.9
	20	5.4	56.5	1.5×10^{-7}	1.05	2.19	2.1
	30	9.1	47.3	3.6×10^{-8}	2.71	7.12	2.6
IV	10	4.2	87.2	1.1×10^{-6}	0.28	0.51	1.8
	20	6.5	78.8	2.2×10^{-7}	0.83	1.99	2.4
	30	15.6	55.2	2.7×10^{-8}	3.28	10.76	3.3